Diffraction-induced edge contrast enhancement for terahertz imaging

Yingxin Wang (王迎新), Ziran Zhao (赵自然)*, Zhiqiang Chen (陈志强), Li Zhang (张 丽), and Kejun Kang (康克军)

Department of Engineering Physics, Tsinghua University, Key Laboratory of Particle and Radiation Imaging (Tsinghua University), Ministry of Education of China, Beijing 100084, China

**E-mail: zhaozr@mail.tsinghua.edu.cn*

Received December 2, 2008

Contrast enhancement is particularly important for imaging of weakly absorbing materials. We demonstrate the inherent contrast-enhancement effect at the edges of a transparent object by using a conventional pulsed terahertz imaging setup without additional modification of the system design. We provide both experimental and theoretical evidence suggesting that this effect is a consequence of the frequency-dependent energy loss of the terahertz radiation induced by edge diffraction. The influence of the phase step of the broadband terahertz pulses on the edge contrast is discussed.

OCIS codes: 110.6795, 050.1940, 120.4290.
doi: 10.3788/COL20090708.0690.

During the past decade, terahertz imaging has attracted considerable interest and undergone remarkable developments both in the system design and in the search for potential applications of this technology[1]. The continuous-wave (CW) terahertz imaging systems have existed for a long time and a variety of related studies were reported recently in parallel with the development of new CW sources, such as backward-wave oscillator, parametric oscillator, and quantum cascade lasers. Pulsed terahertz imaging is another modality evolving from a time-domain spectrometer[2], which allows us to obtain the spectroscopic information about absorption and refraction of an object[3]. On these CW or pulsed systems, applications for nondestructive testing[4,5], material identification[6], and biomedical diagnosis[7] have also been demonstrated.

Complementary to the conventional X-ray and optical imaging techniques, the use of terahertz radiation will generate a relatively high contrast image for common dielectric materials. However, further enhancement of the contrast is essential to improve the image quality and spatial resolution for the inspection of some objects with weak absorption. In terahertz range, methods such as dark-field[8]and phase imaging[9] have been proposed to achieve this purpose. The former exploits the deflected radiation caused by diffraction or scattering of the sample. On the contrary, if only the ballistic signal is detected, it can still provide good contrast. Indeed, this phenomenon has been observed in some standard terahertz imaging setups[4,5], although not following the above hypothesis. Similar to the results of dark-field measurement, the contrast enhancement usually appears at the edge region of the sample, where diffraction of terahertz waves occurs due to the dielectric discontinuity. Therefore, the structure of the sample is visible, benefiting from the presence of edge diffraction.

In this letter, we present a detailed study of the edge diffraction effect in pulsed terahertz imaging. Using a typical time-domain system, we measure the diffraction signal produced by the edge of a nearly nonabsorbing (transparent) object for a focused terahertz beam. Based on Gaussian beam analysis and Huygens-Fresnel principle[10], we perform theoretical calculation of the spatial evolution of the diffracted terahertz pulses for each frequency component in the effective spectral range, and make a comparison with the experimental data.

A commercially available terahertz imaging system (T-Ray 2000, Picometrix, LLC) was used in the experiment. The setup is illustrated in Fig. 1(a), which consists of a fiber-coupled photoconductive transmitter and receiver driven by 100-fs optical pulses from a Ti:sapphire laser at 800 nm, and four silicon lenses with 3-inch focal length for collimating and focusing of the terahertz radiation coupled into (and out of) free space by two aplanatic hyperhemisphere substrate lenses[11]. The beam in the collimated region between lenses L1 and L2 has approximately Gaussian transverse profile with frequency-independent diameter[11] (the measured 1/e radius is ∼10 mm, see Fig. 1(b)). We chose polyethylene (PE) as the testing material, for the reason that it exhibits nearly transparent in terahertz range. As shown in Fig. 1(c), a PE step wedge was fabricated. The step heights are 0.3, 0.5, 1.0, 1.5, and 2.0 mm, respectively, and each one has an area of 10×25 mm^2. We placed the sample in the focal plane, and the terahertz beam transmitted through it at near normal incidence. Then, the sample was mounted on an x-y translation stage and raster scanned to acquire the image data. Nevertheless, considering the one-dimensional (1D) structure, the step wedge was scanned in a single line along the x direction at 0.2-mm intervals. At each spatial point, a time-domain waveform was recorded. Fourier transform of these waveforms yielded the frequency spectra, serving as the major concerns in the following analysis.

We plot the 1D imaging results in Fig. 2, where the intensity represents the spectral amplitude integrated over a specific frequency range, normalized to the reference pulse (corresponding to the scan at position $x = 0$ mm).

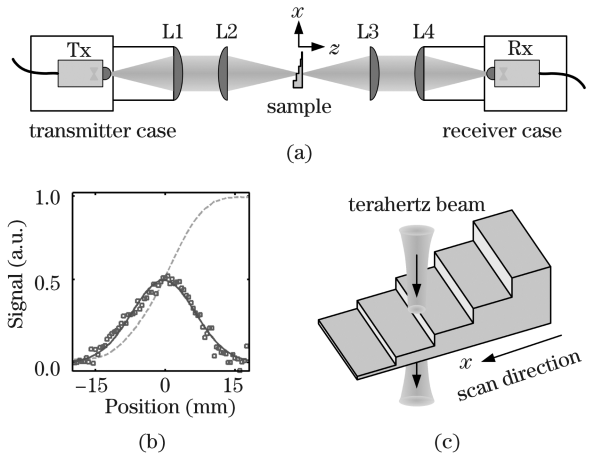

Fig. 1. (a) Terahertz imaging setup. Tx: transmitter; Rx: receiver; L1−L4: Si lenses. (b) Knife-edge scan of the collimated beam (dashed), its derivative (square), and the Gaussian fit (solid). (c) Schematic of the PE step wedge.

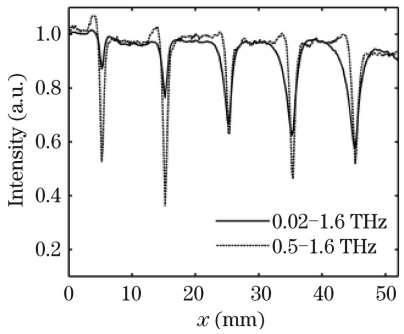

Fig. 2. Terahertz 1D imaging of the PE step wedge. The profiles are formed by integrating the spectral amplitude over two different frequency ranges.

The entire useful range (0.02−1.6 THz) is firstly selected. From the intensity profile, we can observe that the values are relatively low at the five edge positions. This effect gives rise to high contrast for the edges and enables them to be resolved clearly. Because of the transparency of PE, there is no apparent difference between the inside of each step and the background region, not accounting for a slight reflection loss on the sample surface. For a narrower range excluding the low frequencies (0.5−1.6 THz), the edge structure becomes more pronounced and better resolution is obtained as expected. Note that the transmission power increases near the edges, which is possibly attributed to the aperture effect of the detector[8].

The physical origin of the observed contrast enhancement may be understood in terms of electromagnetic wave diffraction by a step discontinuity. Intuitively, when the focused terahertz beam with finite spot size propagates through the edge of the sample, it will experience different phase shifts on both sides of the edge; thus in the transmission region, interference between the two portions of the wave results in a disturbance to the field distribution. Consequently, an abnormal signal is detected. The degree of the field disturbance is wavelength (i.e., phase shift) dependent[12] as we will see by revisiting the above spectroscopic measurements.

Figure 3 shows the two-dimensional (2D) plot of the amplitude spectra as a function of scanning position, normalized to unity. One can find that some characteristic patterns emerge around the edges. The amplitudes of the frequency components associated with these patterns decrease dramatically so as to cause energy loss of the edge signal, as displayed in Fig. 2. In addition, there are more amplitude minima in the spectrum for a thicker edge, which offers a reasonable explanation for the observation that the edge contrast increases with thickness for the integration interval from 0.02 to 1.6 THz (see Fig. 2). Also, according to the locations of these minima, different behaviors of the contrast for the range of 0.5−1.6 THz could be easily explained. Interestingly, the characteristic pattern of an individual edge reveals prominent periodic structure. This is determined by the periodicity of the phase shift. It has been pointed out that the extreme field disturbance takes place while a π-phase step height (the relative phase shift) is induced by the edge[12]. Assuming that the PE wedge acts as a perfectly transparent sample, the phase step height φ corresponding to an edge with a thickness d is given by

$$\varphi = \frac{(n-1)\omega d}{c}, \tag{1}$$

where n represents the refractive index of PE (a measured value of 1.52 is used here), ω is the angular frequency, and c is the speed of light in vacuum. We calculate the frequency values at $\varphi = (2m+1)\pi$ $(m = 0, 1, 2, \cdots)$ for the five edges and mark the corresponding positions with circles in Fig. 3. Good agreement with the distribution of the experimental amplitude minima is achieved. However, there still remains a small discrepancy, probably owing to the imperfect transparency of the sample with the existence of surface reflection and thickness effect. The horizontal dark lines around 1.2 and 1.4 THz which are independent of the scanning position arise from atmospheric water vapor absorption of terahertz waves at specific frequencies[3].

To perform theoretical prediction of the edge diffraction signal, Xi *et al.* used broadband Huygens-Fresnel diffraction integral to calculate the temporal waveform of terahertz pulse at the edge[13], but the exact spatial distribution of the incident beam was not determined, which is not sufficiently accurate for the simulation. Here we simulate the propagation of the terahertz beam using a Gaussian mode and evaluate the field distribution of the diffracted beam based on Huygens-Fresnel principle for each frequency component in the frequency domain. As mentioned above, the emitted radiation after the collimating lens (L1) has a constant beam waist

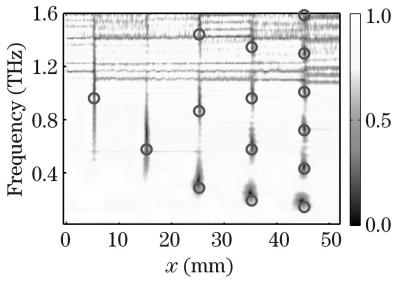

Fig. 3. Normalized amplitude spectra as a function of scanning position and prediction of the positions of the amplitude minima (circles).

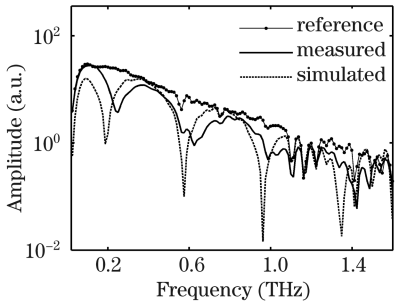

Fig. 4. Diffraction signals of the 1.5-mm-thick edge.

(∼10 mm) for all frequency components. Under this approximation, the spatial evolution of the terahertz beam after the focusing lens (L2) can be described by applying Gaussian-beam transformation. When the step wedge is inserted into the focused beam, it will alter the terahertz field pattern. The diffracted field originates from the sum of two sets of elementary waves with φ-phase difference[12] and can be deduced from Fresnel diffraction integral[14,15]. For the diffraction of a monochromatic Gaussian beam, the field in a plane perpendicular to the propagation direction takes the form

$$\begin{aligned} E(\rho,z) &= -\frac{\mathrm{j}k\exp\left[\mathrm{j}k(z-z_1)\right]}{2\pi(z-z_1)}\int_{-\infty}^{\infty}\mathrm{d}y'\left\{\int_{-\infty}^{0}\mathrm{d}x'E_0(\rho',z_1)\exp(\mathrm{j}\varphi)\exp\left[\mathrm{j}\frac{k(\rho-\rho')^2}{2(z-z_1)}\right]\right. \\ &\quad \left.+\int_{0}^{\infty}\mathrm{d}x'E_0(\rho',z_1)\exp\left[\mathrm{j}\frac{k(\rho-\rho')^2}{2(z-z_1)}\right]\right\} \\ &= \frac{E_0(\rho,z)}{2}\left\{1+\exp(\mathrm{j}\varphi)+\left[1-\exp(\mathrm{j}\varphi)\right](\mathrm{j}-1)F(u)\right\} \quad , \\ F(u) &= \int_0^u \exp(\mathrm{j}\pi t^2/2)\mathrm{d}t \quad , \end{aligned} \tag{2}$$

where $\rho=(x^2+y^2)^{1/2}$ and $\rho'=(x'^2+y'^2)^{1/2}$ are the transverse radial vectors, z and z_1 are the distances from the beam waist to the observation plane and the edge, respectively, $E_0(\rho,z)$ is the field of the initial beam, k is the wave number, $F(u)$ denotes the complex Fresnel integral, and u is the scaled length[15].

In our simulations, we employed the reference spectrum for generating the incident amplitude of each frequency component of the terahertz pulse and calculated the transformed propagation mode (frequency-dependent beam waist size and location) of the focused beam to determine $E_0(\rho,z)$. Then the distribution of the edge diffraction field was obtained straightforwardly from Eq. (2). Furthermore, the effect of the collection optics on this diffraction field was analyzed by accounting for the phase transformation and finite extent of the lens and applying the Fresnel diffraction formula[14]. We treated the field in the plane immediately in front of lens L3 as an input of the collection system and numerically estimated the field in the back focal plane of lens L4 (i.e., the location of the receiving antenna). Figure 4 shows the experimental and simulated results for the 1.5-mm-thick edge exactly located at the beam focus, and the reference spectrum is also given for comparison. Evidently, the measured edge signal is well reproduced by the model. In fact, the simulated spectrum was derived from the field strength at the focus of L4, yielding the amplitude difference from the recorded intensity in the detector which corresponds to the average electric field over the sensitive area. The reason for the discrepancy in minima positions has been discussed above. At low frequencies, the simulation reveals significant strength reduction. This is due to the diffraction at the lens aperture, which has been involved in the calculation and is also present for the reference signal actually.

We note that both the theoretical and experimental results indicate the frequency-dependent diffraction loss for the edge with a given thickness. Since the energy in the paraxial region is significantly reduced owing to destructive interference of the disturbed field for a phase step close to π[12], we get a small signal in the receiver. Such an energy loss leads to the sample edge being highlighted in the resulting image, and the corresponding contrast is dominated by the phase step at the edge. Generally, a thicker edge will be resolved more easily for the full-spectrum integration, while a comparable contrast for a thin edge is likely achieved at some specific frequencies. It should be pointed out that more accurate determination of the diffracted field would require taking into account the influence of reflection and edge thickness, and the vector nature of the fields should also be introduced in the calculation, such as polarization rotation at the edge[16].

In conclusion, we have investigated the edge diffraction effect of transparent objects in terahertz range. For a PE sample, we observed the edge contrast enhancement via a conventional terahertz imaging setup. Theoretical prediction of the diffraction signal agrees well with the experimental measurement. This edge effect extends the potential applications of terahertz imaging, especially for the nondestructive testing of nearly nonabsorbing materials.

This work was supported in part by the Program for New Century Excellent Talents in University (No. NCET-05-0060) and the Fundamental Research Foundation of Tsinghua University (No. JC2007027). The authors thank Dr. Hongfeng Gai and colleagues from Nuctech Company Limited for their helpful conversations.

References

1. W. L. Chan, J. Deibel, and D. M. Mittleman, Rep. Prog. Phys. **70,** 1325 (2007).
2. B. B. Hu and M. C. Nuss, Opt. Lett. **20,** 1716 (1995).
3. Y. Wang, Z. Zhao, Z. Chen, Y. Zhang, L. Zhang, and K. Kang, Opt. Lett. **33,** 1354 (2008).
4. N. Karpowicz, H. Zhong, C. Zhang, K.-I. Lin, J.-S.

Hwang, J. Xu, and X.-C. Zhang, Appl. Phys. Lett. **86,** 054105 (2005).
5. Y. L. Hor, J. F. Federici, and R. L. Wample, Appl. Opt. **47,** 72 (2008).
6. M. Lu, Y. Zhang, J. Sun, S. Chen, N. Li, G. Zhao, and J. Shen, Chin. Opt. Lett. **3,** S239 (2005).
7. S. Nakajima, H. Hoshina, M. Yamashita, C. Otani, and N. Miyoshi, Appl. Phys. Lett. **90,** 041102 (2007).
8. T. Löffler, T. Bauer, K. J. Siebert, H. G. Roskos, A. Fitzgerald, and S. Czasch, Opt. Express **9,** 616 (2001).
9. K. Edward, T. W. Mayes, B. Hocken, and F. Farahi, Opt. Lett. **33,** 216 (2008).
10. M. Born and E. Wolf, *Principles of Optics* (7th edn.) (Cambridge University Press, Cambridge, 1999).
11. J. Van Rudd and D. M. Mittleman, J. Opt. Soc. Am. B **19,** 319 (2002).
12. S. P. Anokhov, J. Opt. Soc. Am. A **24,** 2493 (2007).
13. Z. Xi, X. Yu, and T. Xiao, Chin. Opt. Lett. **6,** 700 (2008).
14. J. W. Goodman, *Introduction to Fourier Optics* (2nd edn.) (McGraw-Hill, New York, 1996).
15. S. Barraza-Lopez, D. F. V. James, and P. G. Kwiat, J. Opt. Soc. Am. A **24,** 1148 (2007).
16. N. C. J. van der Valk, W. A. M. van der Marel, and P. C. M. Planken, Opt. Lett. **30,** 2802 (2005).